Therapeutic Advances in Medical Oncology

Original Research

Combined targeting EGFR and SRC as a potential novel therapeutic approach for the treatment of triple negative breast cancer

Ther Adv Med Oncol

2020, Vol. 12: 1–16

DOI: 10.1177/1758835919897546

Alexandra Canonici, Alacoque L. Browne, Mohamed F. K. Ibrahim, Kevin P. Fanning, Sandra Roche, Neil T. Conlon, Fiona O'Neill, Justine Meiller, Mattia Cremona, Clare Morgan, Bryan T. Hennessy, Alex J. Eustace, Flavio Solca, Norma O'Donovan and John Crown

Abstract

Background: Triple negative breast cancer (TNBC) is an aggressive subtype of breast cancer with limited therapeutic options. Epidermal growth factor receptor (EGFR) has been shown to be over-expressed in TNBC and represents a rational treatment target.

Methods: We examined single agent and combination effects for afatinib and dasatinib in TNBC. We then determined IC_{50} and combination index values using Calcusyn. Functional analysis of single and combination treatments was performed using reverse phase protein array and cell cycle analysis. Finally, we determined the anticancer effects of the combination *in vivo*.

Results: A total of 14 TNBC cell lines responded to afatinib with IC_{50} values ranging from 0.008 to 5.0 μM. Three cell lines, belonging to the basal-like subtype of TNBC, were sensitive to afatinib. The addition of afatinib enhanced response to the five other targeted therapies in HCC1937 and HDQP1 cells. The combination of afatinib with dasatinib caused the greatest growth inhibition in both cell lines. The afatinib/dasatinib combination was synergistic and/or additive in 13/14 TNBC cell lines. Combined afatinib/dasatinib treatment induced G1 cell cycle arrest. Reverse phase protein array results showed the afatinib/dasatinib combination resulted in efficient inhibition of both pERK(T202/T204) and pAkt(S473) signalling in BT20 cells, which was associated with the greatest antiproliferative effects. High baseline levels of pSrc(Y416) and pMAPK(p38) correlated with sensitivity to afatinib, whereas low levels of B-cell lymphoma 2 (Bcl2) and mammalian target of rapamycin (mTOR) correlated with synergistic growth inhibition by combined afatinib and dasatinib treatment. *In vivo*, the combination treatment inhibited tumour growth in a HCC1806 xenograft model.

Conclusions: We demonstrate that afatinib combined with dasatinib has potential clinical activity in TNBC but warrants further preclinical investigation.

Keywords: afatinib, Bcl2, dasatinib, EGFR, TNBC

Received: 28 March 2019; revised manuscript accepted: 6 December 2019.

Correspondence to:
Alex J. Eustace
National Institute for Cellular Biotechnology, Dublin City University, Whitehall, Glasnevin, Dublin 9, Ireland
alex.eustace@dcu.ie

Alexandra Canonici
Alacoque L. Browne
Mohamed F. K. Ibrahim
Kevin P. Fanning
Sandra Roche
Neil T. Conlon
Fiona O'Neill
Justine Meiller
Norma O'Donovan
National Institute for Cellular Biotechnology, Dublin City University, Dublin, Ireland

Mattia Cremona
Clare Morgan
Bryan T. Hennessy
Medical Oncology Group, Department of Molecular Medicine, Beaumont Hospital, Royal College of Surgeons in Ireland, Dublin, Ireland

Flavio Solca
Boehringer Ingelheim RCV GmbH & Co KG, Vienna, Austria

John Crown
National Institute for Cellular Biotechnology, Dublin City University, Dublin, Ireland

Department of Medical Oncology, St Vincent's University Hospital, Dublin, Ireland

Introduction

Triple negative breast cancer (TNBC) is clinically defined as negative for the expression of oestrogen and progesterone receptors, and lacking human epidermal growth factor receptor 2 (HER2) gene amplification, protein overexpression, or both, thereby making it difficult to target therapeutically. With the exception of poly(ADP-ribose) polymerase (PARP) inhibitors for BRCA-mutations in TNBC (approximately 5% of breast cancer cases), the only approved systemic treatment option is chemotherapy.[1] The lack of a proven targeted therapeutic strategy owing to the heterogeneity of TNBC has fostered a major effort to discover molecular targets to treat patients with TNBC. Recently, new treatment

options such as PARP inhibitors, anti-androgen therapies and immune checkpoint inhibitors have emerged.[2] Despite their efficacy, TNBC is a heterogeneous disease and the clinical benefits of these therapies are modest with limited success to date.[2]

Epidermal growth factor receptor (EGFR) is expressed in the majority of TNBC tumours[3] making EGFR inhibitors an attractive treatment option for TNBC patients. Whilst Corkery *et al*. have shown that TNBC cell lines have limited sensitivity to EGFR tyrosine kinase inhibitors (TKIs) gefitinib and erlotinib,[4] combinations of monoclonal antibodies targeting EGFR enhanced growth inhibition of TNBC cells *in vitro* and tumour growth inhibition *in vivo*.[5] Furthermore, clinical data showed that EGFR inhibition in combination with taxane or cisplatin in TNBC provided patients with a longer progression-free survival compared with cisplatin alone.[6,7] Despite the observed limited benefit of EGFR therapy, it should be noted that trials to date have taken place in heavily pretreated, unselected patients. However, a small proportion of patients in these trials have demonstrated response to EGFR inhibitors suggesting that stratifying patients based on EGFR expression may improve outcome. To address the heterogeneity of signalling pathways involved in driving TNBC and the potential mechanisms of resistance to EGFR therapies, it will also be necessary to develop effective combination therapies for appropriately selected subpopulations of patients.

Afatinib, a second-generation irreversible pan-HER TKI,[8] potently suppresses the kinase activity of EGFR and erlotinib-resistant isoforms of the receptor.[9,10] Afatinib can also overcome resistance to cetuximab, a monoclonal antibody targeting EGFR, in a xenograft model of acquired cetuximab resistance.[11] Afatinib displayed potent anti-cancer activity in HER2-positive breast cancer *in vitro*[12] and in clinical trials.[13,14] In addition, afatinib has demonstrated antiproliferative activity in the SUM-149 TNBC cell line *in vitro*.[14] Furthermore, in a clinical trial including 29 TNBC patients, three patients showed stable disease following afatinib therapy for a minimum of 110 days.[15] Therefore, afatinib may be a novel therapeutic strategy in patients with TNBC. However, its effects on TNBC, although promising, have not been thoroughly investigated.

Owing to compensatory signalling pathways, targeting EGFR alone may not be sufficient. There is significant evidence implicating crosstalk between EGFR and proto-oncogene tyrosine-protein kinase Src kinase signalling in both lung cancer and breast cancer.[16–18] In fact, molecular targets including Src have been shown to be key pathways driving TNBC and, as such, hold promise for targeted TNBC treatment. Moreover, TNBC cell lines are more sensitive to the Src inhibitor, dasatinib, than other breast cancer subtypes.[19,20] Studies have shown that afatinib in combination with Src, tyrosine-protein kinase Met (c-Met) and insulin-like growth factor-I receptor (IGF-IR) targeting agents showed synergistic growth response in breast cancer cell lines, including the TNBC cell line MDA-MB-468.[21] In addition, afatinib in combination with dasatinib has been shown to enhance growth suppression *in vitro* and *in vivo* in non-small cell lung cancer[22] and a phase I clinical trial is ongoing (ClinicalTrials.gov identifier: NCT01999985).

TNBC represents a subtype of breast cancer with heterogeneous clinical behaviour, histology and response to therapy.[23,24] Clinical use of targeted drugs in TNBC, including EGFR inhibitors, is hampered by a lack of predictive biomarkers. Therefore, effective selection strategies are necessary to identify patients who are more likely to benefit from the therapies.

In this study, we performed an extensive preclinical evaluation of afatinib, alone and in combination with other targeted therapies, in TNBC *in vitro* and *in vivo*. We also identified predictive biomarkers to select the subset of TNBC patients most likely to benefit from afatinib treatment or combination therapy.

Methods

Reagents

Afatinib (kindly provided by Boehringer Ingelheim GmbH),[10] dasatinib,[25] dovitinib,[26] rapamycin[27] and foretinib[28] (Carbosynth Limited) were prepared as 10 mM stocks in dimethyl sulfoxide [DMSO (Sigma)]; dactolisib (Carbosynth Limited)[29] was prepared as 5 mM stocks in DMSO.

Cells

TNBC cell lines BT20, CAL51, HCC70, HCC1143, HCC1187, HCC1806, HCC1937, Hs578T, MDA-MB-157, MDA-MB-231 and MDA-MB-468 were obtained from the American

A

Drug	Conc	Targets	Reference
Afatinib	1 μM	EGFR, HER2, HER3 & HER4	[25]
Dovitinib	1 μM	FGFR, PDGFR	[27]
Dasatinib	1 μM	SRC, BCR-ABL, c-KIT	[26]
Dactolisib	1 μM	PI3K / mTOR	[30]
Rapamycin	100 nM	mTOR	[28]
Foretinib	1 μM	MET, RON, TEK, AXL, VEGFR	[29]

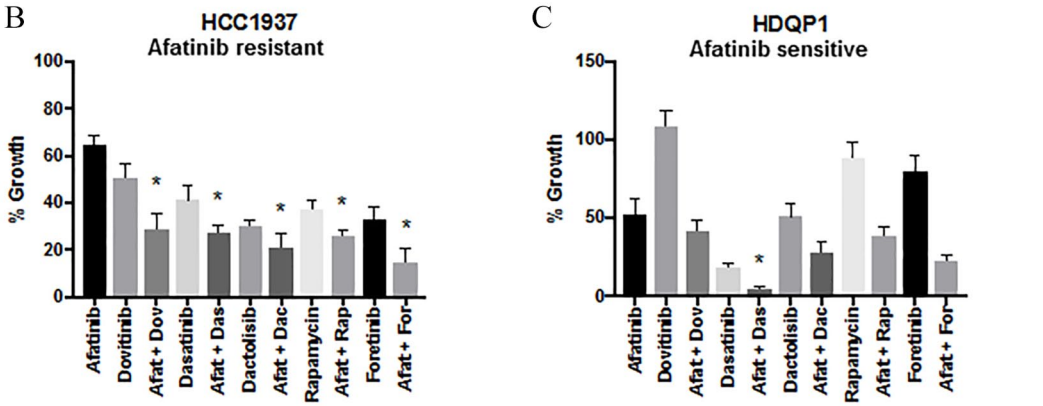

Figure 1. Growth inhibitory effect of afatinib in combination with other targeted therapies. (A) Inhibitors, concentration and relevant targets represented in Table 1. (B) HCC1937 and (C) HDQP1 cells were incubated with afatinib in combination with dovitinib (1:1), dasatinib (1:1), dactolisib (1:1), rapamycin (10:1) or foretinib (1:1) for 5 days. Cell viability was determined using the acid phosphatase method. Data represents the mean ± SEM of three independent replicates.

Tissue Culture Collection (Rockville, MD, USA). TNBC cell lines CAL120, CAL851 and HDQP1 were obtained from the German Tissue Repository DMSZ (Braunschweig, Germany). All cell lines were tested for mycoplasma and authenticated by short tandem repeat (STR) typing (Additional File 1). The HCC1143, HCC1187, HCC1806, HCC1937, Hs578T, MDA-MB-231 and MDA-MB-468 cells were cultured in RPMI (Sigma-Aldrich) containing 10% foetal calf serum (FCS; Life Technologies); the HCC70 cells were cultured in RPMI containing 10% FCS, 1 mM sodium pyruvate (Life Technologies) and 2 mM nonessential amino acids (Life Technologies); the HDQP1 cells were cultured in DMEM (Sigma-Aldrich) containing 10% FCS; the CAL51 cells were cultured in DMEM containing 10% FCS and 1 mM sodium pyruvate; the CAL120 and CAL851 cells were cultured in DMEM (Sigma-Aldrich) containing 10% FCS, 1 mM sodium pyruvate and 2 mM glutamine (Life Technologies); the BT20 cells were cultured in DMEM-HAM F12 (Sigma-Aldrich) containing 10% FCS; the MDA-MB-157 cells were cultured in Leibovitz L15 (Sigma-Aldrich) containing 10% FCS. Cells were incubated at 37°C and 5% CO_2.

Proliferation assays

A total of 5×10^3 cells/well for HCC1187 and MDA-MB-157 cells, 4×10^3 cells/well for CAL851 cells and 3×10^3 cells/well for the other cell lines were seeded in 96-well plates. Following overnight incubation at 37°C, drugs were added at the indicated concentrations and incubated for 5 days at 37°C. For initial combination assays (Figure 1), drugs were mixed at a 1:1 ratio, apart from rapamycin, which was mixed at a 1:10 ratio. For the afatinib and dasatinib combination assays drugs were mixed at 1:5 ratio for all cell lines apart from BT20 and HCC1143 in which drugs were mixed at a 1:20 ratio. Cell proliferation was determined using the acid phosphatase assay as described previously.[30] Inhibition of proliferation was calculated relative to untreated controls. The effective dose of drug that inhibits 50% of growth (IC_{50} values) and combination index (CI) values were determined using the Chou–Talalay equation on CalcuSyn software.[31]

Terminal DNA transferase-mediated dUTP nick end labelling assay

A total of 2.5×10^4 BT20 cells/well were seeded in 24-well plates. Following overnight incubation at 37°C, drugs were added at the indicated concentrations and incubated for 72 h at 37°C. The terminal DNA transferase-mediated dUTP nick end labelling (TUNEL) assay was performed using the Guava TUNEL kit for flow cytometry (Merck Millipore), according to the manufacturer's protocol, as described previously.[32]

Cell cycle analysis by DNA content

A total of 2.5×10^4 BT20 cells/well were seeded in 24-well plates. Following overnight incubation at 37°C, drugs were added at the indicated concentrations and incubated for 72 h at 37°C. The cell cycle assay was performed using the Guava Cell Cycle Reagent for flow cytometry (Merck Millipore), according to the manufacturer's protocol, as described previously.[32] Cells were acquired on the Guava EasyCyte (Merck Millipore), using ModFit LT software for analysis (Verity Software House, Topsham, ME, USA).

Protein extraction for reverse phase protein array

Determination of baseline protein expression. For the BT20, HCC1937 and HDQP1 cell lines, 5×10^5 cells/well were seeded in 6-well plates and allowed to grow until they reached 80% confluence. Cells were washed with phosphate-buffered saline (PBS) and lysed in RPPA lysis buffer (1% Triton X-100, 50 mM HEPES pH 7.4, 150 mM NaCl, 1.5 mM $MgCl_2$, 1 mM EGTA, 100 mM NaF, 10 mM sodium pyrophosphate tetrabasic, 1 mM sodium orthovanadate, 10% glycerol) containing protease (cOmplete, Roche Life Science) and phosphatase (phosSTOP, Roche Life Science) inhibitors. After 20 min incubation on ice, lysate was passed through a 21-gauge needle and centrifuged at 10,000 rpm for 5 min at 4°C. Protein quantification was carried out using the bicinchoninic acid assay (Pierce Biotechnology) and stored at −80°C.

Determination of protein expression following drug treatment. A total of 5×10^5 cells/well were seeded in 6-well plates. Following overnight incubation at 37°C, drugs were added at the indicated concentrations. Following 24 h drug treatment, cells were prepared as described in the previous section.

Reverse phase protein array

A total of 40 µg of proteins were solubilized in sodium dodecyl sulfate (SDS) sample buffer (40% glycerol, 8% SDS, 0.25 M Tris-HCL pH 6.8, 50 mM Bond-Breaker TCEP Solution; Pierce) and heated to 95°C for 5 min. Baseline expression of proteins/phosphorylated proteins of the panel of TNBC cell lines was determined by RPPA as described previously.[33,34] Proteomic profiling of 3 cell lines (BT20, HCC1937 and HDQP1) pre- and post-24 h drug treatment was performed by RPPA following the same procedure.[33,34] The antibodies used are listed in Additional File 2. RPPA analysis was performed as per O'Shea *et al.*[35]

Protein extraction for western blotting

For the BT20s, 2×10^6 cells/well were seeded in 100 mm Petri dishes. After reaching 80% confluence, drugs were added at the indicated concentrations. Following 24 h drug treatment, cells were washed with cold PBS and lysed in RIPA buffer (Sigma-Aldrich) containing a protease inhibitor cocktail (Sigma-Aldrich), 1 mM phenylmethylsulfonyl fluoride (PMSF) and 1 mM sodium orthovanadate. After 20 min incubation on ice, lysate was passed through a 21-gauge needle and centrifuged at 10,000 rpm for 5 min at 4°C. Protein quantification was carried out using the bicinchoninic acid assay (Pierce Biotechnology) and stored at −80°C.

Western blotting

A total of 40 µg of proteins were solubilised in Laemmli sample buffer (250 mM Tris–HCl; 10% SDS; 5% beta-mercaptoethanol; 30% glycerol; 0.02% bromophenol blue), heated to 95°C for 5 min and proteins were separated using Novex 4–12% polyacrylamide gels (Life Technologies). Proteins were transferred to nitrocellulose membrane (Life Technologies). The membrane was blocked with NET buffer (1.5 M NaCl; 0.05 M EDTA; 0.5M Tris pH 7.8; 0.5% Triton X100; 2.5 g/l gelatin) at room temperature for 1 h. After overnight incubation at 4°C with primary antibody (anti-HER2, Calbiochem; anti-p-EGFR (Y1086), Millipore; anti-Src, Upstate; anti-α-tubulin, Sigma; all other antibodies, Cell Signaling Technology, all primary antibodies used at 1:1000). For the Western blotting analysis of the animal tumours, we performed overnight incubation at 4°C with primary antibody (Cyclin D1, p27 Kip1, PARP, cdc42 (CDK1), p-SRC (Y416),

SRC, EGFR (all Cell Signalling Technology); p-EGFR (Y1068) (AbCam) GAPDH (Santa Cruz); all primary antibodies used at 1:1000). Three washes with NET buffer were then carried out, followed by incubation at room temperature protected from light with IRDye secondary antibody (antimouse, LI-COR Biosciences; antirabbit, LI-COR Biosciences, all secondary antibodies used at 1:5000) for 1 h. Following three washes with NET buffer and one PBS wash, infrared fluorescent signals were detected using the Odyssey Imager (LI-COR Biosciences).

In vivo *models*

All *in vivo* work was carried out at Dublin City University (DCU, Dublin, Ireland) approved by DCU Research Ethics Committee (DCUREC/2015/208) and regulated by Health Product Regulatory Authority (HPRA, Dublin, Ireland) under approval number AE19115_P009. All mice were group housed in individually ventilated cages in a specific pathogen free unit and were provided with bedding material, environmental enrichment, and free access to grain-based food pellets and water. The 28- to 35-day-old female CB17/lcr-*Prkdc*^{SCID}/Crl mice (Charles River, UK) were implanted subcutaneously with 5×10^6 HCC1806 cells using a 25 G needle, implanted in 200 µl basal medium/Cultrex Basement Membrane Extract (Amsbio) (1:1 v/v). Animals were randomized to 5 treatment arms 13 days after implantation. Therapeutic agents or vehicle was administered by oral gavage, on a 5 days on, 2 days off regime. The mice were divided into 5 groups as follows: control arm, 100 µl water/mouse; vehicle arm, propylene glycol:water (Sigma-Aldrich) (1/3 v/v) 100 µl/mouse, dasatinib 15 mg/kg prepared in propylene glycol (1:1 v/v) 50 µl/mouse, afatinib 10 mg/kg prepared in water 50 µl/mouse. The combination arm was administered dasatinib, 15 mg/kg and afatinib 10 mg/kg as described, 50 µl of each agent/mouse. Tumour growth was monitored by calliper measurements at least twice per week by a treatment-arm blinded researcher and tumour volume was calculated as $((W \times D \times H)/2)$. Weight changes were also monitored at least twice per week as a marker of overall health. Animals were euthanized by cervical dislocation when a humane endpoint was reached that is, tumour volume exceeded 1600 mm^3, tumour dimension exceeded 15 mm, decline in general health/body condition or loss of skin integrity on tumour.

All tumours were retrieved and snap frozen in liquid nitrogen or formalin fixed, paraffin-embedded for further analysis. Snap frozen tumours were stored at −80°C. Tumours were processed using a tissue micro-dismembrator (Mikro-DisMembrator U, Braun Biotech International), with all parts prechilled with liquid nitrogen to prevent tumours thawing. Tumours were processed to powder at 4000 rpm for minimal time (30–60 s). Powdered tumours were stored at −80°C and protein extracted for Western blotting as described previously.

Immunohistochemistry

To assess EGFR expression in mouse tumour samples, 5 µm sections of formalin-fixed, paraffin-embedded tumours were mounted onto SuperFrost Plus slides (Fisher Scientific) and deparaffinized before antigen retrieval for 20 min at 95°C in Dako PT Link in Target Retrieval Solution pH6 (Dako S1699). Staining was performed on the DAKO AutoStainer. Nonspecific binding was blocked with Real HP Block (DAKO) for 10 min before staining with EGFR (1:200, NovaCastra) for 30 min. Real EnVision (DAKO) secondary was added for 30 min followed by 5 min of Real DAB (DAKO). The samples were counterstained with haematoxylin, dehydrated through grading alcohols 70%, 90% and 100%, cleared in xylene and mounted using DPX mounting medium. For EGFR expression, the whole specimen was examined for the presence or absence of any positive staining following growth *in vivo*.

Statistical analysis

CalcuSyn software (BioSoft) was used to calculate IC_{50} and CI values at 50% effective dose (ED_{50}). A CI value of <0.9 is synergistic, 0.9–1.1 is considered additive and >1.1 is antagonistic. To evaluate combination treatments, a one-way analysis of variance (ANOVA) with Tukey's multiple comparison test was used (GraphPad Prism v.7). To compare the effects of afatinib and dasatinib alone and in combination on protein expression and phosphorylation in our RPPA data, Student's *t* test was used. Correlations between response to afatinib, or the afatinib/dasatinib combination, and potential biomarkers were determined using Spearman-Rank correlation on Graphpad Prism (v.7). Correlation between response to afatinib and the presence of an ErbB

family mutation was assessed using Fisher's exact test (GraphPad Prism v.7). Differences between percentage of apoptotic cells or percentage of cells between each stage of cell cycle pre- and post-treatment were analysed using a two-tailed *t*-test on Excel. $p < 0.05$ was considered statistically significant.

Results

Effect of afatinib in TNBC cell lines

In order to assess the single-agent antiproliferative effects of afatinib, we tested the effect of afatinib on a panel of 14 TNBC cell lines from various triple negative subgroups.[36,37] TNBC cells responded to afatinib with IC_{50} values ranging from 8 nM to >5 μM (Table 1, Additional File 3: Supplemental Figure S1). Defining the peak plasma concentration of afatinib (80 nM) as a cut-off,[38] we identified that 3 of the 7 basal-like cell lines were sensitive to afatinib (MDA-MB-468, CAL851 and HDQP1) whereas none of the non-basal like cell lines were sensitive (Table 1). However, this difference did not achieve statistical significance ($p = 0.07$). Analysis of relevant mutations [ErbB family (EGFR, ErbB2, ErbB3, ErbB4), PIK3CA, TP53, AKT and KRAS] within the TNBC cell lines demonstrated a correlation between the presence of an ErbB mutation and sensitivity to afatinib ($p = 0.01$). Two of the TNBC cell lines tested, HCC1937 and HDQP1, were selected for further investigation as representatives of afatinib resistance and sensitivity, respectively.

Effect of afatinib in combination with other targeted therapies in TNBC cell lines

One of the main difficulties in treating TNBC is the high level of redundancy in survival signalling pathways that impact on growth. Molecular targets including platelet-derived growth factor receptor (PDGFR)/fibroblast growth factor receptor (FGFR),[39] the phosphatidylinositol-4,5-bisphosphate 3-kinase (PI3K)/mTOR pathway,[40] Src and c-Met[41,42] have been shown to be key pathways driving TNBC and, as such, hold promise for targeted TNBC treatment. Therefore, the effect of afatinib was tested in combination with a panel of inhibitors (dovitinib, dasatinib, dactolisib, and foretinib, all 1 μM) and rapamycin (100 nM) to identify possible synergistic therapeutic combinations (Figure 1A). To identify the most effective combination, the targeted therapeutic must exhibit superior growth inhibition than afatinib, and when combined with afatinib must be better than either single agent alone. In HCC1937 cells the combination of afatinib and the five different targeted therapies was significantly more effective at inhibiting growth relative to either drug alone ($p < 0.05$) (Figure 1B). However, in HDQP1 cells, only the combination of afatinib and dasatinib inhibited growth to a higher level relative to either drug alone ($p < 0.05$) (Figure 1C). The percentage growth inhibition and statistical significance for all treatment combinations can be found in Additional File 4. The afatinib/dasatinib combination (5:1) showed antiproliferative activity in HDQP1 (94% growth inhibition) and HCC1937 (70% growth inhibition) and was therefore selected for further investigation in the panel of TNBC cell lines.

Effect of afatinib in combination with dasatinib in TNBC cell lines

Dasatinib, at a peak plasma concentration of 204.9nM,[43] was effective at inhibiting growth in 10 out the 14 TNBC cell lines (Figure 2, Additional File 3: Supplemental Figure S2). The combination of dasatinib with afatinib was synergistic (CI < 0.9) in 6 of the 14 cell lines tested, with BT20, HCC1937 and HDQP1 showing the highest level of synergy (CI 0.04 ± 0.00, 0.12 ± 0.03 and 0.38 ± 0.07, respectively) (Figure 2 and Table 1). In 7 of the 14 cell lines, the combination of afatinib/dasatinib was additive (CI 0.9–1.1), while an antagonistic effect was observed in the CAL120 cell line with the combined treatment (CI 1.32 ± 0.09). Treatment with the combination of afatinib and dasatinib increased sensitivity to afatinib (<80 nM) in HCC1806, HCC1937 and MDA-MB-231 cells (Figure 2 and Additional File 3: Supplemental Figure S2). With this finding, the correlation between TNBC subtype and response to afatinib was reanalysed and found sensitivity to afatinib to be associated with the basal-like subgroups ($p = 0.03$). RPPA analysis of baseline protein expression demonstrated that in the panel of TNBC cell lines, sensitivity to afatinib correlated with higher baseline levels of pSrc (Y416) (Additional File 3: Supplemental Figure S3A, $p = 0.02$, $r = -0.65$) and p38 MAPK (T180/Y182) (Additional File 3: Supplemental Figure S3B, $p = 0.04$, $r = -0.55$). No association was observed between response to afatinib and EGFR expression. Furthermore, low baseline levels of Bcl2

Table 1. Antiproliferative effects of afatinib, alone and in combination with dasatinib in triple negative breast cancer (TNBC) cell lines. TNBC cell lines categorized into TNBC subtypes with ErbB family, TP53, AKT, PIK3CA or KRAS mutations. Cell line mutations identified from ATCC, Broad Institute CCLE and COSMIC databases. Details of cell line IC_{50} values (μM) for afatinib ± SD. Response to afatinib (i.e. sensitivity) defined as IC_{50} value less than the peak plasma (80 nM). Combination index (CI) = synergism, between 0.9 and 1.1 = additivity, and >1.1 = antagonism values at 50% effective dose (ED_{50}) for afatinib and dasatinib in a panel of TNBC cell lines. Response to combination treatment as follows: CI at ED_{50} <0.90.

Cell line	TNBC subtype	Mutation					Afatinib IC_{50} (μM)	Afatinib response	CI at ED_{50}	Afat + Das response
		ErbB family	TP53	AKT	PIK3CA	KRAS				
HCC1143	Basal-like 1	–	p.R248Q	CNV 6.21	–	–	5.03 ± 0.60	Resistant	0.93 ± 0.16	Additivity
HCC1937	Basal-like 1	–	p.R306*	–	–	–	0.90 ± 0.28	Resistant	0.12 ± 0.03	Synergism
MDA-MB-468	Basal-like 1	EGFR – CNV 25.02 HER2 - p.G152fs	p.R273H	–	–	–	0.01 ± 0.00	Sensitive	1.04 ± 0.31	Additivity
CAL851	Basal-like 2	HER4 - p.M1017T	p.K132E	–	–	–	0.01 ± 0.00	Sensitive	0.96 ± 0.13	Additivity
HCC70	Basal-like 2	–	p.R248Q	–	–	–	3.19 ± 0.40	Resistant	0.92 ± 0.30	Additivity
HCC1806	Basal-like 2	–	p.T256fs	–	–	–	0.15 ± 0.05	Resistant	0.55 ± 0.10	Synergism
HDQP1	Basal-like 2	HER3 - p.R967R	p.R213*	–	–	–	0.04 ± 0.01	Sensitive	0.38 ± 0.07	Synergism
CAL51	Mesenchymal-like	–	–	–	p.E542K	–	2.23 ± 0.10	Resistant	1.09 ± 0.05	Additivity
CAL120	Mesenchymal-like	–	Splice site	–	–	–	1.70 ± 0.27	Resistant	1.32 ± 0.09	Antagonism
Hs578T	Mesenchymal stem-like	–	p.V157F	–	–	–	2.66 ± 0.31	Resistant	0.65 ± 0.11	Synergism
MDA-MB-157	Mesenchymal stem-like	–	p.A88fs*52	–	–	–	3.85 ± 0.19	Resistant	0.94 ± 0.24	Additivity
MDA-MB-231	Mesenchymal stem-like	–	p.R280K	–	–	p.G13D	0.54 ± 0.10	Resistant	0.99 ± 0.03	Additivity
HCC1187	Immunomodulatory	–	p.G108del	–	–	–	0.72 ± 0.14	Resistant	0.53 ± 0.20	Synergism
BT20	Unclassified	EGFR – CNV 15.73	p.K132Q	–	p.P539R p.H1047R	–	4.66 ± 0.32	Resistant	0.04 ± 0.00	Synergism

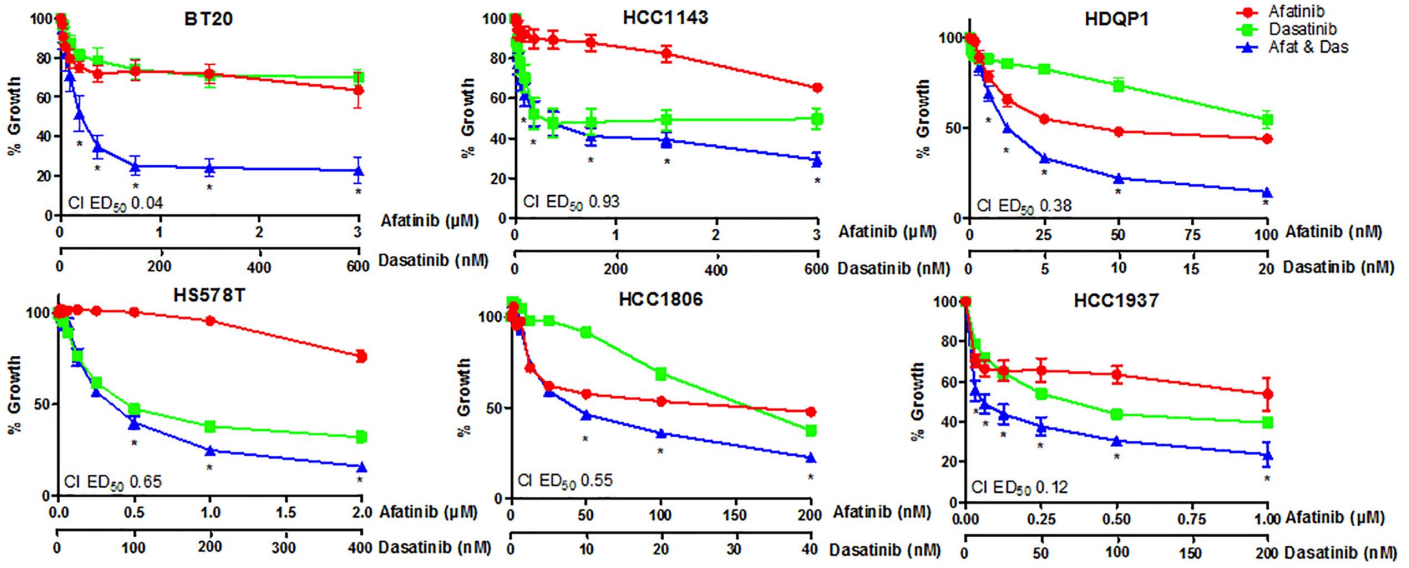

Figure 2. Dose–response effect of afatinib in combination with dasatinib in triple negative breast cancer (TNBC) cell lines. TNBC cell lines were treated with increasing doses of afatinib, dasatinib or the combination at a fixed ratio (5:1) for 5 days. Cell viability was assessed using the acid phosphatase method. Data represents the mean ± SEM of three independent replicates.

(Additional File 3: Supplemental Figure S3C, $p=0.04$, $r=0.57$) and mTOR were predictive of a synergistic response to the afatinib/dasatinib combination (Additional File 3: Supplemental Figure S3D, $p=0.05$, $r=0.54$). All p values for correlation analysis can be found in Additional File 5.

Effect of afatinib in combination with dasatinib on cell signalling

Expression and phosphorylation of PI3K/AKT and Mitogen-activated protein kinase (MAPK)/ERK signalling proteins was interrogated in BT20, HCC1937 and HDQP1 cells following 24 h drug treatment with afatinib, dasatinib or the combination, by RPPA analysis. The three TNBC cell lines were selected as they represent a response range, with BT20 (most synergistic response to afatinib plus dasatinib), HCC1937 (afatinib resistant) and HDQP1 (afatinib sensitive).

Treatment with afatinib alone decreased pEGFR (Y1068) significantly in both BT20 and HCC1937 cells ($p<0.01$ and $p=0.03$) but did not reach significance in HDQP1 cells ($p=0.14$). Afatinib also decreased pAKT (T308) levels significantly in HCC1937 cells (Figure 3B, $p=0.04$).

Across all cell lines, dasatinib treatment decreased pSrc (Y527) levels significantly. Dasatinib alone also decreased pERK1/2 (T202/Y204) signalling significantly in the HDQP1 cells ($p=0.03$) while reducing pAKT (T308) in BT20 cells ($p<0.01$). Interestingly, dasatinib treatment resulted in an increase in the expression of HER2 in all cell lines, however this result did not achieve statistical significance (BT20 $p=0.16$, HCC1937 $p=0.06$, HDQP1 $p=0.09$).

The combination of afatinib and dasatinib significantly decreased pEGFR (Y1068) and pSrc (Y527) across all cell lines. In the BT20 cells, which showed the greatest synergistic response to the combination of afatinib and dasatinib, the combined treatment significantly inhibited both pAKT (S473 and T308), and pMAPK (T202/T204) (Figure 3A, Additional File 3: Supplemental Figure S4). This combined inhibition of pAKT and pMAPK was not observed in either the HCC1937 or HDQP1 cells (Figure 3B and C).

Therefore, to achieve the most synergistic growth inhibition it may be necessary to inhibit both pAKT and pMAPK signalling. All p values for RPPA analysis are provided in Additional File 6.

Effect of afatinib in combination with dasatinib on apoptosis and cell cycle

As the BT20 cells displayed the greatest synergy with afatinib and dasatinib, the effect of the combination treatment on cell cycle and apoptosis was

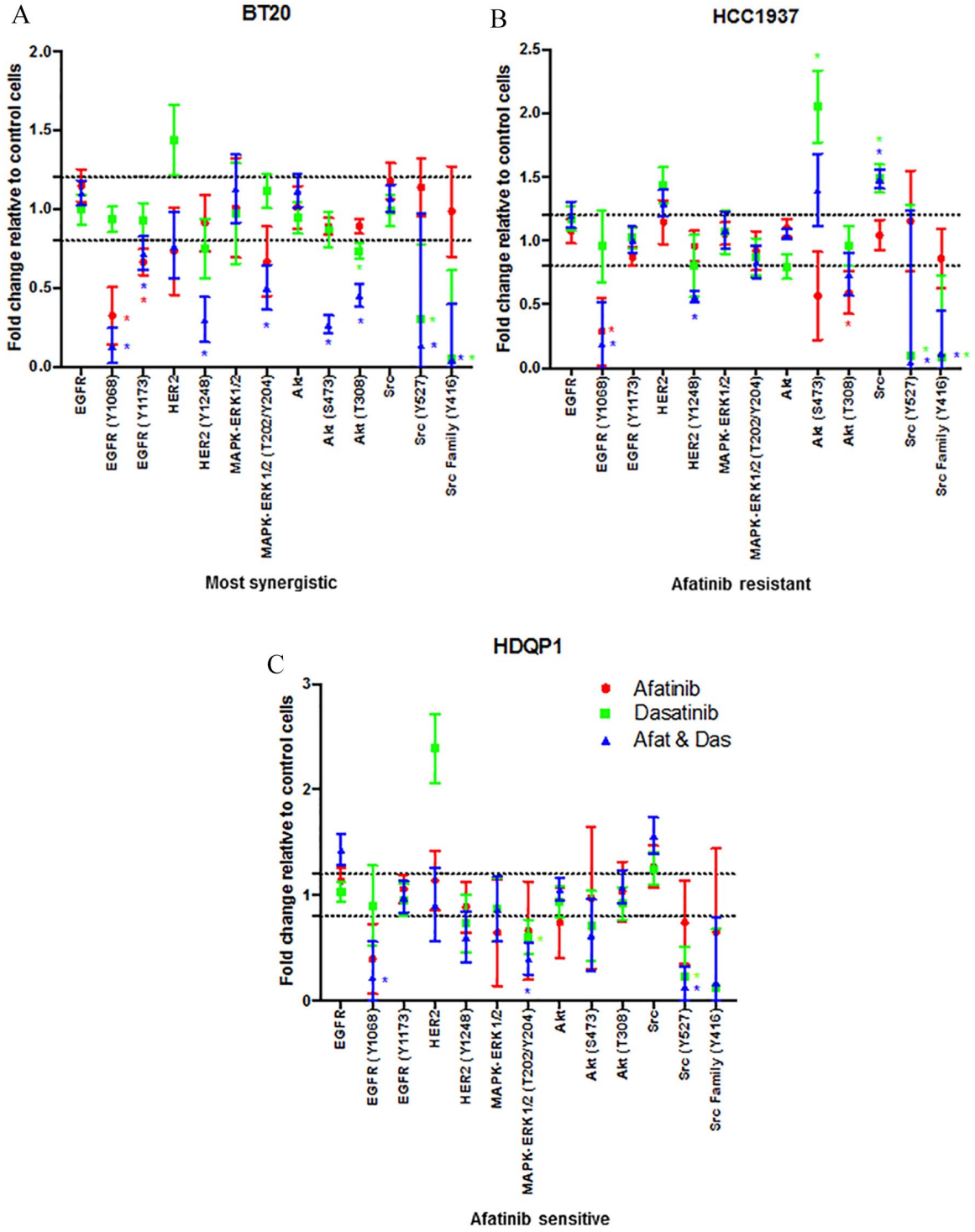

Figure 3. Effect of afatinib and dasatinib, alone and in combination, on cell signalling proteins. (A) BT20, (B) HCC1937 and (C) HDQP1 cells were treated with afatinib (1 μM), dasatinib (200 nM), dasatinib or the combination (5:1) for 24 h. Total protein and phosphorylated protein levels were determined by RPPA. Results displayed as fold-change relative to control treated cells. SEM calculated from three independent protein samples. '*' indicates proteins that have a fold-change of $\geqslant$1.2 fold and a p value of <0.05 as determined by Student's t test.

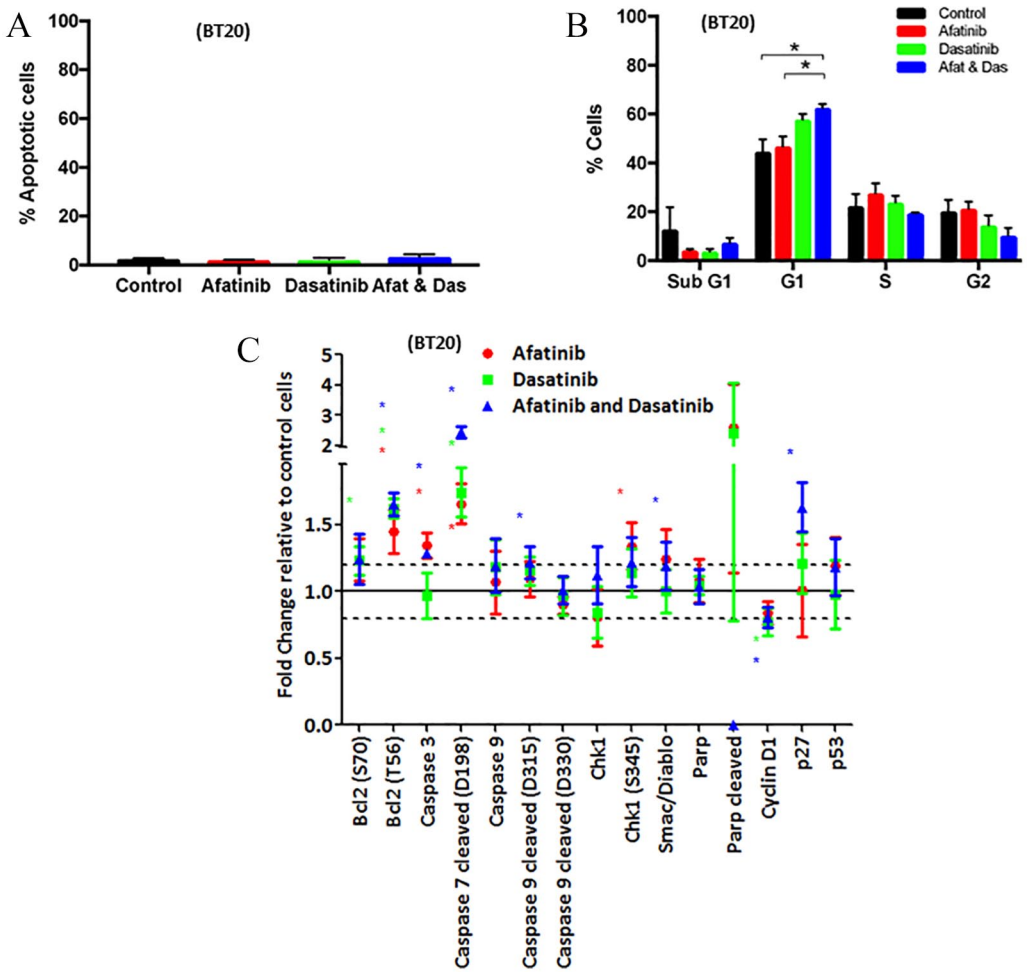

Figure 4. Effect of afatinib and dasatinib, alone and in combination, on apoptosis and cell cycle. (A) BT20 cells were treated with afatinib (3 μM), dasatinib (600nM) or the combination (5:1). Following 72 h of treatment, apoptosis was measured *via* the TUNEL method on the Guava EasyCyte. Data represents the mean ± SEM of three independent replicates. (B) BT20 cells were treated with afatinib, (3 μM), dasatinib (600 nM) or the combination (5:1). Following 72 h of treatment, cell cycle was measured *via* PI staining of DNA content on the Guava EasyCyte. Data represents the mean ± SEM of three independent replicates and $p < 0.05$. (C) BT20 cells were treated with afatinib (1 μM), dasatinib (200 nM) or the combination (5:1) for 24 h. Total protein and phosphorylated protein levels were determined by RPPA. Results displayed as fold-change relative to control treated cells. SEM calculated from three independent protein samples. '*' indicates proteins that have a fold-change of 1.2-fold and a *p* value of < 0.05 as determined by Student's *t* test.

examined in this cell line. After 72 h of treatment with afatinib, dasatinib or the combination, no apoptosis induction was detected by FACS (Figure 4A). Combined afatinib and dasatinib treatment induced significant G1 cell cycle arrest in BT20 cells compared with both control and afatinib alone but not dasatinib alone ($p = 0.01$, $p = 0.04$ and $p = 0.29$, respectively; Figure 4B) by fluorescence-activated cell sorting (FACS). RPPA analysis of phosphorylated and total protein levels following 24 h treatment with afatinib, dasatinib or the combination demonstrated significant changes to both apoptotic and cell cycle proteins (Figure 4C). A 24-hour time point was selected to assess early proteomic alterations associated with changes in apoptosis and cell cycle signalling. Combined treatment induced significant increases in caspase 3, cleaved caspase 7 and 9 and Smac/Diablo suggesting treatment induces a pro-apoptotic effect (Figure 4C, $p < 0.01$, $p < 0.01$, $p = 0.02$ and $p = 0.02$, respectively). Conversely, a significant increase in anti-apoptotic Bcl2 was also demonstrated with treatment, whether alone or in combination (Figure 4C, $p = 0.02$, $p < 0.01$ and $p < 0.01$). However, these changes did not result in an increase in cleaved PARP, indicating they were not sufficient to induce apoptosis in the BT20

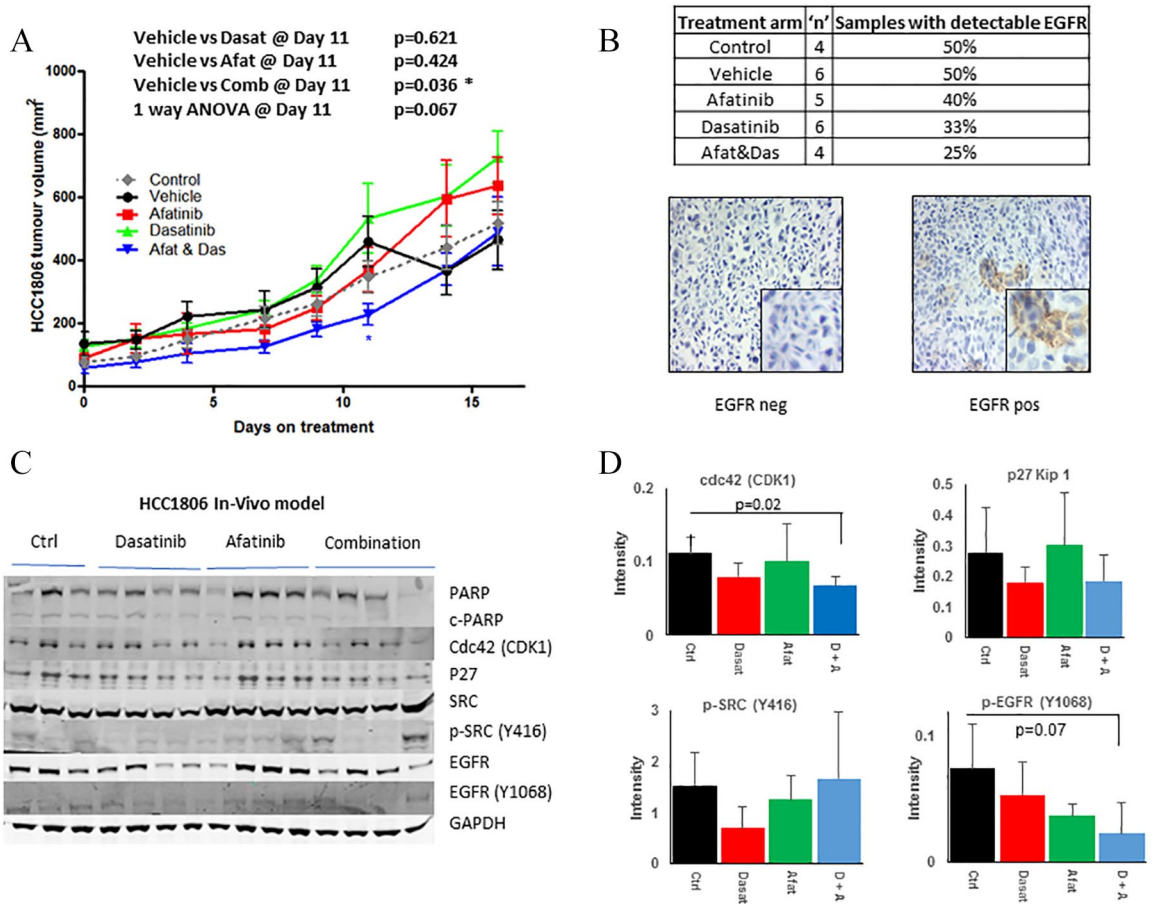

Figure 5. Effect of afatinib and dasatinib, alone and in combination, on tumour growth. (A) HCC1806 cells were implanted by subcutaneous injection into SCID mice. Then 13 days post-implantation, animals were assigned to treatment arms; control, vehicle, afatinib, dasatinib or combination. Growth of the tumour was monitored by calliper measurement. Data was plotted as the average tumour size ± SEM of a minimum of five mice per treatment group. (B) Number of animals with detectable EGFR expression *via* immunohistochemistry. Representative EGFR staining. (C) Total and phosphorylated protein levels were determined by immunoblotting of protein extracted from mouse tumours after completion of *in vivo* study. Relative intensity of cdc42 (CDK1), P27 Kip1, p-SRC (Y416) and p-EGFR (Y1046) as measured by densitometry normalized to GAPDH. Error bars represent the standard deviation of at least triplicate independent experiments. A p value of < 0.05 as calculated by Student's t test was determined as significant.

cells, which corresponds with the FACS analysis. Finally, the combination of afatinib and dasatinib increased levels of p27 with concurrent decreases in cyclin D1 expression suggesting a constraint on progression through cell cycle (Figure 4C, $p < 0.01$ and $p < 0.01$, respectively), which reflects that seen in the FACS analysis.

Assessment of the therapeutic effect of afatinib and dasatinib combination in vivo

We examined the antitumour efficacy of combining afatinib and dasatinib in a xenograft model of HCC1806 cells. HCC1806 cells were chosen as they represent a basal-like TNBC model, which showed synergistic response to afatinib and dasatinib. The combination of afatinib and dasatinib delayed tumour growth relative to the vehicle control with statistical significance achieved following 11 days on treatment ($p = 0.04$). The combination of afatinib and dasatinib showed a trend towards decreased tumour volume relative to all other treatment arms, approaching statistical significance ($p = 0.06$) (Figure 5A) at the end of the experiment. EGFR expression was undetectable, on average, in 60% of the samples and very low in the remaining 40% (Figure 5B) suggesting loss of expression *in vivo* prior to treatment with afatinib. This low EGFR expression may explain the reduced afatinib/dasatinib effect observed *in vivo*.

Western blotting analysis of tumours, taken post-mortem, revealed that treatment with the combination of dasatinib and afatinib resulted in a significant 1.5-fold decrease in cdc42 (CDK1) expression relative to vehicle treated control mice ($p = 0.01$) (Figure 5D). We also observed that treatment with the combination of dasatinib and afatinib resulted in a nonsignificant 1.6-fold decrease in p-EGFR (Y1068) phosphorylation ($p = 0.07$) relative to vehicle control (whilst afatinib alone decreased p-EGFR (Y0168) phosphorylation 1.5-fold, $p = 0.09$). We observed no change in p-SRC (Y416) phosphorylation levels in either dasatinib treated mice ($p = 0.18$), nor those treated with the combination of drugs ($p = 0.17$). However, p-SRC (Y416) levels were higher in two out of the four mice relative to the vehicle-treated control mice.

Discussion

TNBC is characterized by an aggressive phenotype, a high risk of recurrence, and a lack of recognized molecular targets for therapy.[44] Cytotoxic chemotherapy remains the standard of care for TNBC patients. Although randomized trials have established the benefit of adjuvant anthracyclines, taxanes or both in TNBC, long-term prognosis is inferior compared with other subtypes.[45] EGFR is frequently overexpressed in TNBC and its expression is associated with reduced overall survival.[46,47] The question remains whether EGFR is a valid target since many clinical trials investigating the effect of EGFR targeted therapies, including TKIs and monoclonal antibodies, have failed due to low response rates.[48,49] However, these studies have mostly been conducted in heavily pretreated and unselected patient populations.[50] In addition, a small proportion of patients demonstrate response to EGFR inhibitors[50,51] suggesting that stratifying patients may be necessary and subsequent targeting of EGFR may improve outcome. Finally, owing to redundancy in signalling pathways and heterogeneity of the mechanisms of resistance to EGFR therapies, it seems unlikely that treatment of patients with EGFR inhibitors alone will show significant activity clinically. Therefore, it is necessary to develop effective combination therapies for appropriately selected subpopulations of patients. In that regard, our study aims to identify combinations of EGFR and Src kinase TKIs that may provide a better strategy to treat TNBC. However, to achieve this we need to select for TNBC subtypes that are stimulated by the EGFR and SRC pathways.

We tested 14 TNBC cell lines, representing six of the seven characterized triple negative subgroups.[36,37,52] Three cell lines, classified as belonging to the basal-like subtype, showed response to afatinib at clinically achievable concentrations (IC_{50} value < 80 nM). We observed a significant correlation between response to afatinib and expression of pSrc (Y416) and p-p38 MAPK (T180/Y182). Src is both an upstream activator and a downstream mediator of EGFR and has been implicated in development of resistance to EGFR targeted therapies.[53]

The growth inhibitory effects of afatinib were enhanced by combination with all inhibitors tested, most significantly with dasatinib. This result is consistent with other studies that showed a synergistic effect of afatinib and dasatinib in breast cancer, including TNBC, and non-small cell lung cancer.[21,22] Furthermore, afatinib in combination with dasatinib has been shown to overcome acquired afatinib resistance in HER2 positive breast cancer *in vitro*[54] and lung cancer *in vivo*.[55] In this study, we observed the addition of dasatinib with afatinib increased sensitivity to afatinib (at clinically relevant levels) in three afatinib-resistant cell lines (HCC1937, MDA-MB-231 and HCC1806). Low basal expression of the anti-apoptotic protein, Bcl-2, and mTOR correlated with a synergistic response to afatinib/dasatinib combination therapy suggesting that they may be used as predictive biomarkers to select the TNBC patients more likely to respond to treatment. Several clinical studies have shown that high expression of Bcl2 has both poor prognostic and predictive values in TNBC patients.[56–58] Moreover, high expression of mTOR correlates with poor prognosis in early stage TNBC.[59]

RPPA analysis demonstrated that afatinib combined with dasatinib, decreased phosphorylation of both ERK/MAPK and AKT in the BT20 cell line, which showed the strongest synergistic effect in response to the combined treatment. This was the only cell line tested to display this decrease in both ERK/MAPK and PI3K/AKT signalling. Therefore, efficient inhibition of both signalling pathways may contribute to the synergistic antiproliferative effects of the afatinib/dasatinib combined treatment.[60]

Apoptosis and cell cycle analysis suggest that the mechanism of growth inhibition observed with the afatinib/dasatinib combination is predominantly owing to cell cycle arrest rather than induction of cell death. Both afatinib and dasatinib

have previously been described to individually induce G1 cell cycle arrest in the HER2-positive breast cancer cell line SKBR3.[21] While we observed an increase in caspase-3, -7, and -9 protein signalling by RPPA analysis, apoptosis was not induced, at the timepoint tested (RPPA at 24 h *versus* apoptosis at 72 h). This may be due to the concurrent increase in Bcl2 thereby blocking successful execution of apoptosis.[61–64] Addition of a Bcl2 targeted therapy to the combination may further enhance the effect of the combination therapy and ensure cytotoxic activity.

The basal-like cell line HCC1806 showed the best response to the combination treatment at lower concentrations of afatinib and are known to produce tumours in mice.[65] Therefore, they were selected for the *in vivo* study. Combined afatinib and dasatinib treatment resulted in a significant decrease in tumour growth relative to the vehicle control ($p = 0.036$) and a nonsignificant decrease ($p = 0.067$; one-way ANOVA) in tumour volume when compared with the vehicle control, single-agent dasatinib and afatinib. The nonsignificant decrease in tumour growth resulting from the combination of afatinib and dasatinib relative to single therapy could be due to the modest synergy observed *in vitro*, or due to the low frequency of EGFR expression *in vivo* observed (which has been reported previously[66]) that may reduce the impact of afatinib. In support of our *in vitro* findings, analysis of the tumours identified that combined treatment with afatinib and dasatinib resulted in a significant decrease in CDK1 expression; a result which reinforces our *in vitro* observation that the combination of drugs induces cell cycle arrest. However, we observed from Western blotting analysis of the tumours (taken at day 21 and 23 of treatment) that p-SRC (Y416) levels were elevated in two of the mice four treated with the combination of dasatinib and afatinib. Therefore, despite initial anticancer activity at day 11, the combination of afatinib and dasatinib may be limited in the HCC1806 cell line owing to the development of acquired resistance.

Conclusion

In summary, the combination of afatinib/dasatinib displays positive results *in vitro*, achieving synergy in several TNBC cell lines. Afatinib sensitivity was associated with a basal-like phenotype in the panel of TNBC cell lines and correlated with high pSrc and pMAPK levels. Low Bcl2 and mTOR may be predictive biomarkers for a synergistic response to afatinib/dasatinib combination. The cytostatic effect of combinatorial treatment observed *in vitro* was also seen in *in vivo* tumours. Our study has demonstrated that afatinib combined with dasatinib has potential clinical activity in TNBC, but warrants further preclinical investigation before progressing to clinical trials.

Acknowledgements

The authors would like to thank Patricia Gaule, Deirdre Winrow, Laura Ivers, Alejandra Estepa Fernandez, Ian Martin, Ines Kaupe, Karin Bosch, Daniel Zach and Alika Cotton for their technical assistance with this project. The opinions, findings and conclusions or recommendations expressed in this material are those of the author(s) and do not necessarily reflect the views of the Irish Cancer Society.

Author contributions

AC, AE, FS, NOD and JC provided the overall design of the experiments. SR, NTC, FON and JM performed the *in vivo* experiments. MC, CM, BTH assisted with RPPA analysis. AC, MFKI and KPF helped with functional assays. AB, AE and AC performed all data analysis. AB, AC and AJE wrote the manuscript. All authors read and approved the final manuscript.

Funding

The author(s) disclosed receipt of the following financial support for the research, authorship, and/or publication of this article: The authors acknowledge support from Boehringer Ingelheim, the Cancer Clinical Research Trust, the Irish Cancer Society (BREAST-PREDICT, grant number CCRC13GAL), Irish Research Council (Enterprise Partnership Scheme Postdoctoral Fellowship) and the Health Research Board (HRB Summer Student Scholarship).

Conflict of interest statement

Alexandra Canonici, John Crown and Norma O'Donovan received research funding from Boehringer Ingelheim (BI). Flavio Solca is a BI employee.

Ethics approval

All *in vivo* work was carried out at Dublin City University (DCU, Dublin, Ireland) approved by DCU Research Ethics Committee (DCUREC/2015/208) and regulated by Health Product Regulatory Authority (HPRA, Dublin, Ireland) under approval number AE19115_P009.

ORCID iD
Alex J. Eustace https://orcid.org/0000-0002-4092-1360

Availability of data and material

The datasets used and/or analysed during the current study are available from the corresponding author on reasonable request.

Supplemental material

Supplemental material for this article is available online.

References

1. Robson M, Im SA, Senkus E, *et al.* Olaparib for metastatic breast cancer in patients with a germline BRCA mutation. *N Engl J Med* 2017; 377: 523–533.
2. Lee A and Djamgoz MBA. Triple negative breast cancer: emerging therapeutic modalities and novel combination therapies. *Cancer Treat Rev* 2018; 62: 110–122.
3. Dent R, Trudeau M, Pritchard KI, *et al.* Triple-negative breast cancer: clinical features and patterns of recurrence. *Clin Cancer Res* 2007; 13: 4429–4434.
4. Corkery B, Crown J, Clynes M, *et al.* Epidermal growth factor receptor as a potential therapeutic target in triple-negative breast cancer. *Ann Oncol* 2009; 20: 862–867.
5. Ferraro DA, Gaborit N, Maron R, *et al.* Inhibition of triple-negative breast cancer models by combinations of antibodies to EGFR. *Proc Natl Acad Sci U S A* 2013; 110: 1815–1820.
6. Baselga J, Gómez P, Greil R, *et al.* Randomized phase II study of the anti-epidermal growth factor receptor monoclonal antibody cetuximab with cisplatin versus cisplatin alone in patients with metastatic triple-negative breast cancer. *J Clin Oncol* 2013; 31: 2586–2592.
7. Nechushtan H, Vainer G, Stainberg H, *et al.* A phase 1/2 of a combination of cetuximab and taxane for "triple negative" breast cancer patients. *Breast* 2014; 23: 435–438.
8. Awada AH, Dumez H, Hendlisz A, *et al.* Phase I study of pulsatile 3-day administration of afatinib (BIBW 2992) in combination with docetaxel in advanced solid tumors. *Invest New Drugs* 2013; 31: 734–741.
9. Li D, Ambrogio L, Shimamura T, *et al.* BIBW2992, an irreversible EGFR/HER2 inhibitor highly effective in preclinical lung cancer models. *Oncogene* 2008; 27: 4702–4711.
10. Solca F, Dahl G, Zoephel A, *et al.* Target binding properties and cellular activity of afatinib (BIBW 2992), an irreversible ErbB family blocker. *J Pharmacol Exp Ther* 2012; 343: 342–350.
11. Quesnelle KM and Grandis JR. Dual kinase inhibition of EGFR and HER2 overcomes resistance to cetuximab in a novel in vivo model of acquired cetuximab resistance. *Clin Cancer Res* 2011; 17: 5935–5944.
12. Canonici A, Ivers L, Conlon NT, *et al.* HER-targeted tyrosine kinase inhibitors enhance response to trastuzumab and pertuzumab in HER2-positive breast cancer. *Invest New Drugs*. Epub ahead of print 30 July 2018. DOI: 10.1007/s10637-018-0649-y.
13. Geuna E, Montemurro F, Aglietta M, *et al.* Potential of afatinib in the treatment of patients with HER2-positive breast cancer. *Breast Cancer (Dove Med Press)* 2012; 4: 131–137.
14. Hurvitz SA, Shatsky R and Harbeck N. Afatinib in the treatment of breast cancer. *Expert Opin Investig Drugs* 2014; 23: 1039–1047.
15. Schuler M, Awada A, Harter P, *et al.* A phase II trial to assess efficacy and safety of afatinib in extensively pretreated patients with HER2-negative metastatic breast cancer. *Breast Cancer Res Treat* 2012; 134: 1149–1159.
16. Zhang J, Kalyankrishna S, Wislez M, *et al.* SRC-family kinases are activated in non-small cell lung cancer and promote the survival of epidermal growth factor receptor-dependent cell lines. *Am J Pathol* 2007; 170: 366–376.
17. Irwin ME, Bohin N and Boerner JL. SRC-family kinases mediate epidermal growth factor receptor signaling from lipid rafts in breast cancer cells. *Cancer Biol Ther* 2011; 12: 718–726.
18. Irby RB and Yeatman TJ. Role of Src expression and activation in human cancer. *Oncogene* 2000; 19: 5636–5642.
19. Tryfonopoulos D, Walsh S, Collins DM, *et al.* SRC: a potential target for the treatment of triple-negative breast cancer. *Ann Oncol* 2011; 22: 2234–2240.
20. Finn RS, Dering J, Ginther C, *et al.* Dasatinib, an orally active small molecule inhibitor of both the src and abl kinases, selectively inhibits growth of basal-type/"triple-negative" breast cancer cell lines growing in vitro. *Breast Cancer Res Treat* 2007; 105: 319–326.

21. Stanley A, Ashrafi GH, Seddon AM, *et al.* Synergistic effects of various Her inhibitors in combination with IGF-1R, C-MET and SRC targeting agents in breast cancer cell lines. *Sci Rep* 2017; 7: 3964.
22. Yoshida T, Zhang G, Smith MA, *et al.* Tyrosine phosphoproteomics identifies both codrivers and cotargeting strategies for T790M-related EGFR-TKI resistance in non-small cell lung cancer. *Clin Cancer Res* 2014; 20: 4059–4074.
23. Criscitiello C, Azim HA Jr, Schouten PC, *et al.* Understanding the biology of triple-negative breast cancer. *Ann Oncol* 2012; 23(Suppl. 6): vi13–vi18.
24. Reddy KB. Triple-negative breast cancers: an updated review on treatment options. *Curr Oncol* 2011; 18: e173–e179.
25. O'Hare T, Walters DK, Stoffregen EP, *et al.* In vitro activity of Bcr-Abl inhibitors AMN107 and BMS-354825 against clinically relevant imatinib-resistant Abl kinase domain mutants. *Cancer Res* 2005; 65: 4500–4505.
26. Renhowe PA, Pecchi S, Shafer CM, *et al.* Design, structure-activity relationships and in vivo characterization of 4-amino-3-benzimidazol-2-ylhydroquinolin-2-ones: a novel class of receptor tyrosine kinase inhibitors. *J Med Chem* 2009; 52: 278–292.
27. Edwards SR and Wandless TJ. The rapamycin-binding domain of the protein kinase mammalian target of rapamycin is a destabilizing domain. *J Biol Chem* 2007; 282: 13395–13401.
28. Qian F, Engst S, Yamaguchi K, *et al.* Inhibition of tumor cell growth, invasion, and metastasis by EXEL-2880 (XL880, GSK1363089), a novel inhibitor of HGF and VEGF receptor tyrosine kinases. *Cancer Res* 2009; 69: 8009–8016.
29. Maira SM, Stauffer F, Brueggen J, *et al.* Identification and characterization of NVP-BEZ235, a new orally available dual phosphatidylinositol 3-kinase/mammalian target of rapamycin inhibitor with potent in vivo antitumor activity. *Mol Cancer Ther* 2008; 7: 1851–1863.
30. Canonici A, Gijsen M, Mullooly M, *et al.* Neratinib overcomes trastuzumab resistance in HER2 amplified breast cancer. *Oncotarget* 2013; 4: 1592–1605.
31. Reynolds CP and Maurer BJ. Evaluating response to antineoplastic drug combinations in tissue culture models. *Methods Mol Med* 2005; 110: 173–183.
32. Mahgoub T, Eustace AJ, Collins DM, *et al.* Kinase inhibitor screening identifies CDK4 as a potential therapeutic target for melanoma. *Int J Oncol* 2015; 47: 900–908.
33. Hennessy BT, Lu Y, Gonzalez-Angulo AM, *et al.* A technical assessment of the utility of reverse phase protein arrays for the study of the functional proteome in non-microdissected human breast cancers. *Clin Proteomics* 2010; 6: 129–151.
34. Stemke-Hale K, Gonzalez-Angulo AM, Lluch A, *et al.* An integrative genomic and proteomic analysis of PIK3CA, PTEN, and AKT mutations in breast cancer. *Cancer Res* 2008; 68: 6084–6091.
35. O'Shea J, Cremona M, Morgan C, *et al.* A preclinical evaluation of the MEK inhibitor refametinib in HER2-positive breast cancer cell lines including those with acquired resistance to trastuzumab or lapatinib. *Oncotarget* 2017; 8: 85120–85135.
36. Lehmann BD, Bauer JA, Chen X, *et al.* Identification of human triple-negative breast cancer subtypes and preclinical models for selection of targeted therapies. *J Clin Invest* 2011; 121: 2750–2767.
37. Lehmann BD, Jovanović B, Chen X, *et al.* Refinement of triple-negative breast cancer molecular subtypes: implications for neoadjuvant chemotherapy selection. *PLoS One* 2016; 11: e0157368.
38. Wind S, Schmid M, Erhardt J, *et al.* Pharmacokinetics of afatinib, a selective irreversible ErbB family blocker, in patients with advanced solid tumours. *Clin Pharmacokinet* 2013; 52: 1101–1109.
39. Sharpe R, Pearson A, Herrera-Abreu MT, *et al.* FGFR signaling promotes the growth of triple-negative and basal-like breast cancer cell lines both in vitro and in vivo. *Clin Cancer Res* 2011; 17: 5275–5286.
40. Yunokawa M, Koizumi F, Kitamura Y, *et al.* Efficacy of everolimus, a novel mTOR inhibitor, against basal-like triple-negative breast cancer cells. *Cancer Sci* 2012; 103: 1665–1671.
41. Gastaldi S, Comoglio PM and Trusolino L. The Met oncogene and basal-like breast cancer: another culprit to watch out for? *Breast Cancer Res* 2010; 12: 208.
42. Gaule PB, Crown J, O'Donovan N, *et al.* cMET in triple-negative breast cancer: is it a therapeutic target for this subset of breast cancer patients? *Expert Opin Ther Targets* 2014; 18: 999–1009.
43. Demetri GD, Lo Russo P, MacPherson IR, *et al.* Phase I dose-escalation and pharmacokinetic study of dasatinib in patients with advanced solid tumors. *Clin Cancer Res* 2009; 15: 6232–6240.

44. Denkert C, Liedtke C, Tutt A, *et al*. Molecular alterations in triple-negative breast cancer-the road to new treatment strategies. *Lancet* 2017; 389: 2430–2442.

45. Carey LA, Dees EC, Sawyer L, *et al*. The triple negative paradox: primary tumor chemosensitivity of breast cancer subtypes. *Clin Cancer Res* 2007; 13: 2329–2334.

46. Nielsen TO, Hsu FD, Jensen K, *et al*. Immunohistochemical and clinical characterization of the basal-like subtype of invasive breast carcinoma. *Clin Cancer Res* 2004; 10: 5367–5374.

47. Viale G, Rotmensz N, Maisonneuve P, *et al*. Invasive ductal carcinoma of the breast with the "triple-negative" phenotype: prognostic implications of EGFR immunoreactivity. *Breast Cancer Res Treat* 2009; 116: 317–328.

48. Heinemann V, Stintzing S, Kirchner T, *et al*. Clinical relevance of EGFR- and KRAS-status in colorectal cancer patients treated with monoclonal antibodies directed against the EGFR. *Cancer Treat Rev* 2009; 35: 262–271.

49. Pirker R, Pereira JR, Szczesna A, *et al*. Cetuximab plus chemotherapy in patients with advanced non-small-cell lung cancer (FLEX): an open-label randomised phase III trial. *Lancet* 2009; 373: 1525–1531.

50. von Minckwitz G, Jonat W, Fasching P, *et al*. A multicentre phase II study on gefitinib in taxane- and anthracycline-pretreated metastatic breast cancer. *Breast Cancer Res Treat* 2005; 89: 165–172.

51. Schuler M, Fischer JR, Grohé C, *et al*. Experience with afatinib in patients with non-small cell lung cancer progressing after clinical benefit from gefitinib and erlotinib. *Oncologist* 2014; 19: 1100–1109.

52. Bareche Y, Venet D, Ignatiadis M, *et al*. Unravelling triple-negative breast cancer molecular heterogeneity using an integrative multiomic analysis. *Ann Oncol* 2018; 29: 895–902.

53. Boerner JL. Role of SRC family kinases in acquired resistance to EGFR therapies in cancer. *Cancer Biol Ther* 2009; 8: 704–706.

54. Conlon NT, Canonici A, Morgan C, *et al*. Targeting SRC kinase blocks development of afatinib resistance in HER2-positive breast cancer. *Cancer Res* 2018; 78(Suppl. 4): abstract P4-03-15.

55. Booth L, Roberts JL, Tavallai M, *et al*. The afatinib resistance of in vivo generated H1975 lung cancer cell clones is mediated by SRC/ERBB3/c-KIT/c-MET compensatory survival signaling. *Oncotarget* 2016; 7: 19620–19630.

56. Abdel-Fatah TM, Perry C, Dickinson P, *et al*. Bcl2 is an independent prognostic marker of triple negative breast cancer (TNBC) and predicts response to anthracycline combination (ATC) chemotherapy (CT) in adjuvant and neoadjuvant settings. *Ann Oncol* 2013; 24: 2801–2807.

57. Bouchalova K, Svoboda M, Kharaishvili G, *et al*. BCL2 is an independent predictor of outcome in basal-like triple-negative breast cancers treated with adjuvant anthracycline-based chemotherapy. *Tumour Biol* 2015; 36: 4243–4252.

58. Choi JE, Kang SH, Lee SJ, *et al*. Prognostic significance of Bcl-2 expression in non-basal triple-negative breast cancer patients treated with anthracycline-based chemotherapy. *Tumour Biol* 2014; 35: 12255–12263.

59. Ueng SH, Chen SC, Chang YS, *et al*. Phosphorylated mTOR expression correlates with poor outcome in early-stage triple negative breast carcinomas. *Int J Clin Exp Pathol* 2012; 5: 806–813.

60. Jahangiri A and Weiss WA. It takes two to tango: dual inhibition of PI3K and MAPK in rhabdomyosarcoma. *Clin Cancer Res* 2013; 19: 5811–5813.

61. Blagosklonny MV. Unwinding the loop of Bcl-2 phosphorylation. *Leukemia* 2001; 15: 869–874.

62. Cory S and Adams JM. The BCL2 family: regulators of the cellular life-or-death switch. *Nat Rev Cancer* 2002; 2: 647–656.

63. Czabotar PE, Lessene G, Strasser A, *et al*. Control of apoptosis by the BCL-2 protein family: implications for physiology and therapy. *Nat Rev Mol Cell Biol* 2014; 15: 49–63.

64. Dimmeler S, Breitschopf K, Haendeler J, *et al*. Dephosphorylation targets Bcl-2 for ubiquitin-dependent degradation: a link between the apoptosome and the proteasome pathway. *J Exp Med* 1999; 189: 1815–1822.

65. Volk-Draper LD, Rajput S, Hall KL, *et al*. Novel model for basaloid triple-negative breast cancer: behaviour in vivo and response to therapy. *Neoplasia* 2012; 14: 926–942.

66. Keller PJ, Lin AF, Arendt LM, *et al*. Mapping the cellular and molecular heterogeneity of normal and malignant breast tissues and cultured cell lines. *Breast Cancer Res* 2010; 12: R87.